



**University of
Zurich**^{UZH}

**Zurich Open Repository and
Archive**

University of Zurich
Main Library
Strickhofstrasse 39
CH-8057 Zurich
www.zora.uzh.ch

Year: 2012

Proteomic surfaceome analysis of mesothelioma

Ziegler, A; Cerciello, F; Bigosch, C; Bausch-Fluck, D; Felley-Bosco, E; Ossola, R; Soltermann, A; Stahel, R A; Wollscheid, B

Abstract: Identification of new markers for malignant pleural mesothelioma (MPM) is a challenging clinical need. Here, we propose a quantitative proteomics primary screen of the cell surface exposed MPM N-glycoproteins, which provides the basis for the development of new protein-based diagnostic assays. Using the antibody-independent mass-spectrometry based cell surface capturing (CSC) technology, we specifically investigated the N-glycosylated surfaceome of MPM towards the identification of protein-marker candidates discriminatory between MPM and lung adenocarcinoma (ADCA). Relative quantitative CSC analysis of MPM cell line ZL55 in comparison with ADCA cell line Calu-3 revealed a bird's eye view of their respective surfaceomes. In a secondary screen of fifteen MPM and six ADCA, we used high throughput low density microarrays (LDAs) to verify specificity and sensitivity of nineteen N-glycoproteins overregulated in the surfaceome of MPM. This proteo-transcriptomic approach revealed thy-1/CD90 (THY1) and teneurin-2 (ODZ2) as protein-marker candidates for the discrimination of MPM from ADCA. Thy-1/CD90 was further validated by immunohistochemistry on frozen tissue sections of MPM and ADCA samples. Together, we present a combined proteomic and transcriptomic approach enabling the relative quantitative identification and pre-clinical selection of new MPM marker candidates.

DOI: <https://doi.org/10.1016/j.lungcan.2011.07.009>

Posted at the Zurich Open Repository and Archive, University of Zurich

ZORA URL: <https://doi.org/10.5167/uzh-53099>

Journal Article

Accepted Version

Originally published at:

Ziegler, A; Cerciello, F; Bigosch, C; Bausch-Fluck, D; Felley-Bosco, E; Ossola, R; Soltermann, A; Stahel, R A; Wollscheid, B (2012). Proteomic surfaceome analysis of mesothelioma. *Lung Cancer*, 75(2):189-196.

DOI: <https://doi.org/10.1016/j.lungcan.2011.07.009>

1 Proteomic Surfaceome Analysis of Mesothelioma

2
3 Annemarie Ziegler^{*,1,†}, Ferdinando Cerciello^{*,1,3}, Colette Bigosch^{1,‡}, Damaris Bausch-
4 Fluck³, Emanuela Felley-Bosco¹, Reto Ossola³, Alex Soltermann², Rolf A. Stahel¹,
5 Bernd Wollscheid³

6
7 ¹Clinic of Oncology, and ²Institute for Surgical Pathology, University Hospital
8 Zürich, 8044 Zürich, Switzerland

9 ³Institute of Molecular Systems Biology, Swiss Federal Institute of Technology
10 (ETH), 8093 Zürich, Switzerland

11
12 *AZ and FC contributed equally to this work

13
14 [†]Present address: Centro de Genética Humana, Clínica Alemana-Universidad del
15 Desarrollo, Santiago, Chile

16 [‡]Present address: Umweltmikrobiologie, EAWAG, Dübendorf, Switzerland

17 Correspondence to

18
19 Dr. Bernd Wollscheid
20 ETH Zürich, Institute of Molecular Systems Biology (IMSB)
21 HPT D77, Wolfgang-Pauli-Strasse 16
22 CH-8093 Zürich
23 Phone: +41 44 633 36 84
24 Fax: +41 44 633 10 51
25 E-Mail: bernd.wollscheid@imsb.biol.ethz.ch

26
27 Dr. med. Ferdinando Cerciello
28 ETH Zürich, Institute of Molecular Systems Biology (IMSB)
29 HPT E52, Wolfgang-Pauli-Strasse 16
30 CH-8093 Zürich
31 Phone: +41 44 633 68 56
32 Fax: +41 44 633 10 51
33 E-Mail: cerciello@imsb.biol.ethz.ch

34 **Abstract**

35 The identification of new markers for malignant pleural mesothelioma (MPM) is a
36 challenging clinical need. Here, we propose a quantitative proteomics primary screen
37 of the cell surface exposed MPM N-glycoproteins, which provide the basis for the
38 development of new protein-based diagnostic assays. Using the antibody-independent
39 mass-spectrometry based cell surface capturing (CSC) technology, we specifically
40 investigated the N-glycosylated surfaceome of MPM towards the identification of
41 protein-marker candidates discriminatory between MPM and lung adenocarcinoma
42 (ADCA). Relative quantitative CSC analysis of MPM cell line ZL55 in comparison
43 with ADCA cell line Calu-3 revealed a bird's eye view of their respective
44 surfaceomes. In a secondary screen of fifteen MPM and six ADCA, we used high
45 throughput Low Density Microarrays (LDAs) to verify specificity and sensitivity of
46 nineteen N-glycoproteins overregulated in the surfaceome of MPM. This proteo-
47 transcriptomic approach revealed thy-1/CD90 (THY1) and teneurin-2 (ODZ2) as
48 protein-marker candidates for the discrimination of MPM from ADCA. Thy-1/CD90
49 was further validated by immunohistochemistry on frozen tissue sections of MPM and
50 ADCA samples. Together, we present a combined proteomic and transcriptomic
51 approach enabling the relative quantitative identification and pre-clinical selection of
52 new MPM marker candidates.

53

54 **Keywords:** Mesothelioma, Surfaceome, Cell Surface Capturing (CSC)
55 technology, N-glycoproteins, Surface markers, CD90, ODZ2.

56

57

58

59 **1. Introduction**

60 Malignant pleural mesothelioma (MPM) is an aggressive disease mainly caused by
61 asbestos exposure [1]. The diagnosis requires immunohistochemistry (IHC),
62 combining panels of antibodies against MPM markers (positive for MPM) like
63 calretinin, podoplanin (clone D2-40), cytokeratins 5/6 or WT-1 together with
64 carcinoma-markers (negative for MPM) like epithelial cell adhesion molecule (Ep-
65 CAM, clone Ber-EP4), carcinoembryonic antigen (CEA) or thyroid transcription
66 factor-1 (TTF-1). However, the discrimination of MPM from other malignancies
67 affecting the lung can be difficult. Particularly, the distinction between MPM and
68 lung adenocarcinoma (ADCA) is most challenging [3]. Recently, antibody-
69 independent approaches have evolved as alternative tools for the discrimination of the
70 two diseases, based on gene expression-ratios, RT-PCR or DNA-methylation profiles
71 [4-7]. Despite promising laboratory-based results, the translation of similar techniques
72 into clinical routine remains problematic [8-10].

73 Here, we propose a combined proteomic and transcriptomic strategy for the
74 identification and selection of new protein-markers for the discrimination between
75 MPM and ADCA. First, we applied the recently developed mass-spectrometry (MS)
76 based cell surface capturing (CSC) technology [11] towards the discovery of the N-
77 glycosylated surfaceome of MPM and ADCA cells. Thereafter, we used the higher
78 throughput Low Density Microarray (LDA) technique, to assess MPM specificity of
79 selected N-glycoproteins on a larger panel of MPM and ADCA cell lines. Our
80 approach revealed thy-1/CD90 (THY1) and teneurin-2 (ODZ2) as new MPM marker
81 candidates. Using a commercially available antibody, we verified thy-1/CD90
82 expression in tumor samples by IHC, showing that results from our proteo-
83 transcriptomic approach can potentially be directly translated into diagnostic routine.

84 **2. Materials and Methods**

85 **2.1. Cell culture**

86 Primary MPM cell cultures were derived from tumor specimens obtained at the time
87 of surgery from patients at the University Hospital Zürich with a confirmed diagnosis,
88 or were derived from MPM malignant pleural-effusions, as previously described [12].
89 The study was approved by the Ethics Committee of the University Hospital Zürich
90 and written informed consent was obtained from all patients. Primary tumor cultures
91 were characterized by immunodetection of the MPM markers mesothelin, calretinin,
92 wt-1, podoplanin (clone D2-40), N-cadherin and vimentin. MPM cell lines MSTO-
93 211H, H2052, H2452 and H226 were from American Type Culture Collection ATCC
94 (Manassas, VA), ZL55 was established in our laboratory [13]. MPM cells were
95 cultured as described before [12]. The ADCA cell lines Calu-3, A549, Calu-6, SK-
96 LU-1 and the adeno-squamous lung cancer cell line H596 were from ATCC, ZL25
97 was established in our laboratory [14]. ADCA cells were cultured in RPMI-1640
98 (Gibco/Invitrogen) with 10% FCS, 2 mM L-glutamine, 1% (w/v)
99 penicillin/streptomycin. All cell lines were maintained at 37°C in a humidified
100 atmosphere with 5% CO₂.

101 **2.2. Cell Surface Capturing (CSC) and mass-spectrometric analysis**

102 SILAC labelling, CSC and mass spectrometric analysis of the MPM cell line ZL55
103 and the ADCA cell line Calu-3 were performed as previously described [11] [15].
104 Heavy-Lysine and heavy-Arginine (L-Lysine-¹³C₆, ¹⁵N₂ and L-Arginine-¹³C₆, ¹⁵N₄,
105 Sigma) were used according to the manufacturer's instructions. All MS/MS spectra
106 were converted to mzXML and searched against the UniProt database (Version 57.15)

107 using the SEQUEST algorithm. Statistical data-analysis was performed using a
108 combination of ISB (Institute of Systems Biology, Seattle) open-source software tools
109 (PeptideProphetTM, ProteinProphetTM, TPP version 4.3.1;
110 <http://tools.proteomecenter.org/software.php>). A ProteinProphet protein probability
111 score of at least 0.9 was used for data-filtering, followed by manual validation.
112 Quantitative SILAC data analysis was performed using the XPRESS software [16,
113 17]. Data was imported, stored, annotated and validated within the in-house developed
114 SISYPHUS database software.

115 **2.3. Low Density Arrays (LDAs)**

116 Cell lines were grown to ~80% confluence in 25 cm² flasks, and total RNA was
117 isolated using the RiboPure kit (Ambion, Austin, TX) as indicated by the
118 manufacturer. RNAs were recovered in 50 µl elution buffer and concentrations
119 determined by spectrophotometric measurement in a NanoDrop ND-1000 (Thermo
120 Scientific, Wilmington, DE) device. For synthesis of cDNA, 750 ng total RNA were
121 reverse-transcribed using the High-Capacity cDNA Reverse-Transcription kit
122 (Applied Biosystems, Foster City, CA) in a total volume of 30 µl, following the
123 manufacturer's instructions. This amount had been experimentally determined to
124 warrant synthesis of cDNA and subsequent amplification by real-time PCR under
125 non-saturated, linear conditions. The quality of cDNA was verified by PCR
126 amplification of a β2-microglobulin fragment in 50 µl reactions containing 2 µl
127 cDNA, 1x Buffer II (Applied Biosystems), 1.5 mM MgCl₂, 0.13 µM each primer, 0.2
128 mM each dATP, dTTP, dCTP, and dGTP, and 1.25 units AmpliTaq Gold (Applied
129 Biosystems). Amplification conditions were: 1 cycle at 95°C for 6 min, 35 cycles at
130 95°C for 45 seconds, 60°C for 1 min, and 72°C for 30 sec, followed by one final cycle

131 at 72°C for 10 min. Primer sequences were: β 2-F, 5'-
132 GTGGAGCATTTCAGACTTGTCTTTCAGC-3', and β 2-R, 5'-
133 TTCATCCAATCCAAATGCGGCATCTTC-3'. PCR products were visualized by
134 electrophoresis on polyacrylamide gels. Low Density Arrays for analysis of 22 genes
135 (three internal controls) were obtained from Applied Biosystems. Each LDA slot was
136 loaded with 100 μ l solution containing 1x Universal Master Mix (Applied
137 Biosystems) and 10 μ l cDNA. PCR amplification was performed in a 7900HT Fast
138 Real-Time PCR System (Applied Biosystems) apparatus using following cycle
139 conditions: 1 cycle of 50°C for 2 min, 1 cycle of 94°C for 10 min, and 40 cycles of
140 97°C for 30 sec, 60°C for 1 min. Relative gene expression was calculated by using the
141 $2^{-\Delta\Delta C_t}$ method [18]. For each sample, three technical replicates were measured and
142 averaged before performing calculation. 18s and GAPDH were used as internal
143 references.

144 **2.4. Western blot**

145 Detection of mesothelin and N-cadherin was performed on the MPM cell line ZL55
146 and the ADCA cell line Calu-3 by Western blot as previously described [12].
147 Detection of thy-1/CD90 was performed without reducing agents on RIPA-buffer
148 (Upstate Biotech-Millipore, Lake Placid, NY) lysates of the MPM cell lines ZL55 and
149 SDM5, and the ADCA cell lines Calu-3 and SK-LU-1, using a monoclonal anti-thy-1
150 antibody (clone AS02, - Dianova, Hamburg, Germany) at 1:5000 dilution [19]. For
151 sample deglycosylation, cell lysates were incubated overnight with 5 U/mg PNGaseF
152 (Roche, Basel, Switzerland) at 37°C.

153 **2.5. Immunofluorescent staining.**

154 Immunofluorescent staining was performed on the ZL55 MPM cells and the Calu-3
155 ADCA cells after fixation with 4% paraformaldehyde and permeabilization with 0.1%
156 TritonX-100 on uncoated coverslips. Antibody clone 5E10 (BD-Pharmingen, San
157 Diego, CA) was used at 1:100 dilution for thy-1/CD90 detection. Mouse IgG1 κ at
158 1:100 (BD-Pharmingen) was used as specificity isotype-control. Cells were
159 counterstained with Alexa Fluor-488-conjugated cholera-toxin (Invitrogen) at 1:5000
160 dilution and DAPI (Sigma-Aldrich) at 1:1000 dilution. Images were acquired by
161 confocal laser-scanning microscopy on a TCS-SPE microscope (Leica Microsystems,
162 Wetzlar, Germany) at 63x magnification and processed (brightness and contrast
163 adjustments and necessary cropping) using the Java-based program ImageJ (National
164 Institute of Health, <http://rsb.info.nih.gov/ij/>).

165 **2.6. Tissue samples and immunohistochemistry**

166 Fresh frozen human tumor specimens were obtained from the Biobank at the Institute
167 for Surgical Pathology, University Hospital Zürich. Corresponding formalin-fixed,
168 paraffin-embedded tumor tissues were processed and diagnoses reported according to
169 the guidelines of the Swiss Society of Pathology. Immunohistochemistry was
170 performed on ice-cold, acetone fixed, frozen whole sections of 5 μ m thickness after
171 endogenous peroxidase quenching. Thy-1/CD90 detection was performed using the
172 antibody-clone 5E10 (BD-Pharmingen) at 1:20 dilution and the Vectastain Elite ABC
173 Universal Kit (Vector Laboratories) according to the manufacturer's instructions.
174 Immunoreactivity was visualized by incubation with 3,3'-diaminobenzidine
175 tetrahydrochloride (Vector Laboratories) followed by counterstaining with
176 haematoxylin QS (Vector laboratories). Mouse IgG1 κ (BD-Pharmingen) at 1:20 was

177 used as specificity isotype-control. For each sample, stroma staining-intensity was
178 used as internal reference.

179 **3. Results**

180 **3.1. SILAC-based CSC proteomic analysis of N-glycosylated surface proteins**

181 In order to identify differences in-between the surfaceomes of MPM and ADCA we
182 used a SILAC-based CSC proteomic strategy (Fig. 1). The MPM cell line ZL55 and
183 the ADCA cell line Calu-3 were grown in media containing heavy or light isotope
184 forms of the aminoacids arginine and lysine, respectively (SILAC protocol) [20]. The
185 incorporation of different aminoacid isotopes allows to mix the two cell types in equal
186 amounts before lysis and to process them together. MS discrimination between MPM-
187 derived proteins (containing heavy forms of arginine and lysine) and ADCA proteins
188 (containing light forms of arginine and lysine) is then possible based on the mass
189 differences of the incorporated heavy and light peptide isoforms. Following the CSC
190 protocol, the sugar moieties of the cell surface exposed glycoproteins are labelled
191 with biotin hydrazide on the living cells and, after protein digestion with trypsin, the
192 glycopeptides are enriched with streptavidin coated beads. Using the enzyme
193 PNGaseF, N-glycosylated peptides are then specifically released and analyzed via
194 microfluidic LC-MS/MS. Overall, 100 cell surface N-glycoproteins, including 37 CD
195 annotated proteins, were identified (Supplementary Table ST1). The MS analysis also
196 revealed 211 MPM/ADCA N-glycopeptides containing a deamidation signature
197 within the NXS/T motif, indicating the specific isolation and PNGaseF-mediated
198 release of those N-glycopeptides via CSC (Supplementary Table ST2). We thereafter
199 used the software XPRESS to calculate abundance ratios between the MPM and
200 ADCA proteins. Among the glycoproteins upregulated in MPM, we identified the

201 known MPM markers mesothelin (UniProt ID MSLN_human, Q13421; Entrez gene
202 name MSLN) and N-cadherin (synonyms CD325, Cadherin-2; UniProt ID
203 CADH2_human, P19022; Entrez gene name CDH2) (Fig. 2A) The clear upregulation
204 of the two proteins detected by MS in ZL55 (mesothelin abundance-ratio calculated
205 with the software XPRESS revealed a ratio of ADCA over MPM of 0.04 ± 0.00 and
206 for N-cadherin an abundance-ratio of 0.05 ± 0.04) matched the results obtained by
207 Western blot (WB) (Fig. 2B), confirming the specificity of our approach.

208 **3.2. Semi-quantitative RT-PCR cell lines screening for MPM cell surface** 209 **glycoprotein-marker candidates**

210 In the next set of experiments, we used LDAs in order to further qualify the initial
211 MPM glycoprotein markers at the transcription level on a larger panel of
212 representative and diverse MPM and ADCA cell lines (Table 1). The mRNA
213 expression of 19 pre-qualified N-glycoproteins from the proteomic screen, including
214 mesothelin and N-cadherin as landmark proteins, was analyzed in fifteen MPM and
215 six ADCA cell lines (Fig. 3 and supplementary table ST3). Mesothelin transcript was
216 expressed in ten out of fifteen (67%) MPM cell lines and in the adeno-squamous cell
217 line H596. N-cadherin was expressed in all (100%) MPM and also in three (50%)
218 ADCA cell lines. Among the other investigated genes, thy-1/CD90 (synonym CD90;
219 UniProt ID THY1_human, P04216; Entrez gene name THY1) and teneurin-2
220 (UniProt ID TEN2_human, Q9NT68; Entrez gene name ODZ2) displayed a selective
221 association with MPM (Fig. 3A and B). Thy-1/CD90 (THY1) showed homogenous
222 mRNA expression in MPM and was absent from ADCA cell lines. Teneurin-2
223 (ODZ2) was expressed in eleven MPM cell lines, but only at low levels in one ADCA
224 (SK-LU-1) and one adeno-squamous cell line (H596). All other candidates presented

225 a heterogeneous expression profile without individual discriminatory power between
226 MPM and ADCA.

227 **3.3. Western blot verification of thy-1 in MPM and ADCA cell lines**

228 As a first step to verify our markers by immunologic assays, we tried to acquire
229 suitable antibodies. Since no antibody for human teneurin-2 was commercially
230 available, we generated a rabbit anti-serum against two extracellular peptides
231 identified in the proteomic screens from teneurin-2. However, no specific signals
232 could be detected in WB and IHC experiments (data not shown). For thy-1/CD90, we
233 tested a series of commercially available antibodies (data not shown) and selected the
234 mouse clone AS02 to compare thy-1/CD90 expression in two MPM (ZL55, SDM5)
235 and two ADCA (Calu-3, SK-LU-1) cell lines by WB (Fig. 4). Chemoluminescent
236 signals of the appropriate molecular weight were obtained for deglycosylated thy-
237 1/CD90 in MPM cells (lane 6 and 8), but not in ADCA cells (lane 2 and 4). Only in
238 the MPM SDM5 cell line, thy-1/CD90 protein was also recognized in its
239 glycosylated, higher molecular weight form (lane 7).

240 **3.4. Immunohistochemical verification of thy-1 in human tissues**

241 We further set out to validate our proteo-transcriptomic approach in IHC assays. In
242 our hands, the anti-thy-1 clone AS02 did not perform satisfactory on tissues (data not
243 shown), thus, we tested additional commercially available antibodies and selected the
244 clone 5E10. It has to be mentioned that none of the tested antibodies did perform on
245 formalin-fixed paraffin-embedded (FFPE) tissues (data not shown). In agreement with
246 MS, RT-PCR and WB results, using clone 5E10, thy-1/CD90 expression was detected
247 in MPM, but not in ADCA cell lines (Fig. 5A). The overlay of a cholera-toxin

248 staining for the plasma membrane associated ganglioside GM1 with anti-thy-1
249 staining suggests a co-localisation of both molecules at the cell surface. We further
250 used clone 5E10 to investigate human frozen sections from four epithelioid and two
251 biphasic MPM tumors as well as eight ADCA with different grading levels (Fig. 5B,
252 supplementary table ST4). Reaction to anti-thy-1 antibody was observed in the tumor-
253 stromal cells of both tumor types. Three MPM cases presented discrete numbers of
254 tumor cells with moderate membrane staining whereas ADCA cells reacted only
255 modestly, if at all, to anti-thy-1 with weak to moderate cytoplasmic staining of tumors
256 cells toward the stroma.

257 **4. Discussion**

258 In our work we investigated a new approach to the analysis of the MPM surfaceome
259 toward the identification of markers for the discrimination of MPM from ADCA. To
260 do so, we analyzed the surfaceomes of two MPM and ADCA cell lines via the CSC
261 technology. The CSC technology enables the parallel identification of surface
262 exposed N-glycosylated proteins using antibody-independent mass spectrometric
263 techniques. The CSC technology thus allows for large screens of proteins without
264 biases related to antibody availability or quality. To sort for N-glycoproteins
265 associated with MPM, we combined the CSC with the SILAC strategy for relative
266 protein quantitation and selected those proteins showing upregulation in MPM
267 compared to ADCA. The validity of this approach was corroborated by the unbiased
268 detection of the glycoproteins mesothelin and N-cadherin among the proteins with
269 higher abundance in MPM. Both proteins are in fact known to be associated with
270 MPM, even if their specificity is unsatisfactory for clinical application [21-23]. In
271 addition, MS observed overregulation of the two proteins in MPM could be

272 reproduced and confirmed by antibody-assays (WB). However, it should be
273 mentioned that we could not observe the widely accepted MPM markers calretinin,
274 podoplanin, cytokeratins 5/6 or WT-1. This was due to the fact that these protein-
275 markers are neither cell surface exposed (with the exception of podoplanin) nor N-
276 glycosylated, and thus not accessible by our approach.

277 Among the N-glycoproteins upregulated in MPM, we focused on those
278 proteins, which were only rarely or not at all reported in the literature in association
279 with MPM before. In order to anticipate the MPM specificity and sensitivity of these
280 selected proteins, we screened fifteen MPM and six ADCA cell lines by LDAs assays.
281 We decided to apply LDAs, owing to the fact that RT-PCR protocols are nowadays
282 standardized, quick, easily accessible and relatively cheap compared to current
283 proteomic approaches. In contrast to screens based solely on mRNA investigations,
284 here we could take advantage of our previous MS analysis, selecting only for genes
285 known to be translated in proteins. Again, to confirm the validity of the approach, we
286 first looked at our landmarks proteins mesothelin and N-cadherin. As expected, none
287 of the two proteins resulted to be a reliable single discriminator for MPM [21-23].
288 Among the other investigated genes, thy-1/CD90 (THY1) and teneurin-2 (ODZ2)
289 showed the strongest association with MPM. Teneurin-2 (ODZ2) is one of the four
290 members of the teneurin family of proteins. These more than 300 kDa large
291 transmembrane proteins are probably involved in cell-signalling and transcription
292 regulation, but their function is yet unknown [24]. Only few studies report about
293 teneurin-2 in cancer and there is some uncertainty about its potential tumor-
294 suppressor or oncogenic function [25, 26]. Since no commercial antibodies against
295 human teneurin-2 were available, we produced rabbit-antisera against two
296 extracellular peptide sequences. However, reaction of the antibody was

297 unsatisfactory. Thy-1/ CD90 (THY1) is a small, heavily glycosylated GPI-anchored
298 cell surface protein with the highest expression in human among (primarily fetal)
299 thymic stromal cells and most fibroblasts [27]. A tumor-suppressor function of thy-
300 1/CD90 has been proposed in ovarian and nasopharyngeal cancer [28-32], but protein
301 expression in cancer stem-cells has rather been associated with more aggressive
302 behaviour and chemoresistance [33-35]. Recently, thy-1/CD90 has been observed in
303 four MPM cell cultures grown in low serum conditions and a correlation to highly-
304 proliferative or stem-cell-like cells was speculated by the authors [36].

305 We used WB to validate MPM specificity of thy-1/CD90 at protein level.
306 Interestingly, in one MPM case (cell line ZL55), thy-1/CD90 was detectable only
307 after deglycosylation with PNGaseF, pointing out a clear pitfall of approaches based
308 solely on antibodies. Finally, we verified thy-1/CD90 expression in MPM and ADCA
309 tissues by IHC on frozen sections. Three MPM patients presented discrete numbers of
310 tumor cells reacting positively to anti-thy-1 antibody (clone 5E10), while ADCA
311 tumor cells reacted rather weakly and unspecific to the antibody. However, both
312 tumors showed positive reaction of the tumor-stromal cells. To further verify and
313 confirm these preliminary observations in larger scale, suitable antibodies for
314 paraffin-embedded tissues would be essential.

315 **5. Conclusions**

316 Our work investigated a novel proteo-transcriptomic strategy for the identification of
317 MPM biomarkers discriminatory from ADCA. Cell surface analysis with the CSC
318 technology in combination with LDAs enabled the high-throughput and multiplexed
319 screen required for the investigation and pre-clinical selection of new biomarkers.
320 This strategy resulted to be a valid complement to approaches based solely on

321 antibodies, whose limitations are often related to epitope and application-based
322 constraints. Our results provide evidence that teneurin-2, and especially thy-1/CD90,
323 are cell surface accessible marker candidates for the differentiation of MPM from
324 ADCA.

325 **Acknowledgements**

326 This work was supported by the Cancer League of Zürich and the NCCR Neural
327 Plasticity and Repair of the Swiss National Science Foundation (SNF). F.C. is
328 recipient of a fellowship under the MD-PhD programme of the SNF and student at the
329 MD-PhD and Cancer Biology programs of the University of Zürich. We thank
330 Thomas Bock, Andreas Frei and Hansjörg Möst for fruitful discussion and Dr.
331 Marianne Tinguely and Dr. Andreas Hofmann for critical reading of a draft
332 manuscript.

333 **Conflict of interest statement**

334 Authors declare no conflicting financial interests.

335

336

337

338

339

340

341

342

343

344 **References**

- 345 1. Berry G, Newhouse ML, Wagner JC. Mortality from all cancers of asbestos
346 factory workers in east London 1933-80. *Occup Environ Med* 2000; 57: 782-
347 785.
- 348 2. Husain AN, Colby TV, Ordonez NG, Krausz T, Borczuk A, Cagle PT,
349 Chirieac LR, Churg A, Galateau-Salle F, Gibbs AR, Gown AM, Hammar SP,
350 Litzky LA, Roggli VL, Travis WD, Wick MR. Guidelines for pathologic
351 diagnosis of malignant mesothelioma: a consensus statement from the
352 International Mesothelioma Interest Group. *Arch Pathol Lab Med* 2009; 133:
353 1317-1331.
- 354 3. Roberts F, McCall AE, Burnett RA. Malignant mesothelioma: a comparison of
355 biopsy and postmortem material by light microscopy and
356 immunohistochemistry. *J Clin Pathol* 2001; 54: 766-770.
- 357 4. Gordon GJ, Jensen RV, Hsiao LL, Gullans SR, Blumenstock JE, Ramaswamy
358 S, Richards WG, Sugarbaker DJ, Bueno R. Translation of microarray data into
359 clinically relevant cancer diagnostic tests using gene expression ratios in lung
360 cancer and mesothelioma. *Cancer Res* 2002; 62: 4963-4967.
- 361 5. Holloway AJ, Diyagama DS, Opeskin K, Creaney J, Robinson BW, Lake RA,
362 Bowtell DD. A molecular diagnostic test for distinguishing lung
363 adenocarcinoma from malignant mesothelioma using cells collected from
364 pleural effusions. *Clin Cancer Res* 2006; 12: 5129-5135.
- 365 6. Christensen BC, Marsit CJ, Houseman EA, Godleski JJ, Longacker JL, Zheng
366 S, Yeh RF, Wrensch MR, Wiemels JL, Karagas MR, Bueno R, Sugarbaker
367 DJ, Nelson HH, Wiencke JK, Kelsey KT. Differentiation of lung
368 adenocarcinoma, pleural mesothelioma, and nonmalignant pulmonary tissues
369 using DNA methylation profiles. *Cancer Res* 2009; 69: 6315-6321.
- 370 7. Gordon GJ. Transcriptional profiling of mesothelioma using microarrays.
371 *Lung Cancer* 2005; 49 Suppl 1: S99-S103.
- 372 8. Michiels S, Koscielny S, Hill C. Prediction of cancer outcome with
373 microarrays: a multiple random validation strategy. *Lancet* 2005; 365: 488-
374 492.
- 375 9. Draghici S, Khatri P, Eklund AC, Szallasi Z. Reliability and reproducibility
376 issues in DNA microarray measurements. *Trends Genet* 2006; 22: 101-109.
- 377 10. Pollack JR. A perspective on DNA microarrays in pathology research and
378 practice. *Am J Pathol* 2007; 171: 375-385.
- 379 11. Wollscheid B, Bausch-Fluck D, Henderson C, O'Brien R, Bibel M, Schiess R,
380 Aebersold R, Watts JD. Mass-spectrometric identification and relative
381 quantification of N-linked cell surface glycoproteins. *Nat Biotechnol* 2009;
382 27: 378-386.
- 383 12. Thurneysen C, Opitz I, Kurtz S, Weder W, Stahel RA, Felley-Bosco E.
384 Functional inactivation of NF2/merlin in human mesothelioma. *Lung Cancer*
385 2009; 64: 140-147.
- 386 13. Schmitter D, Lauber B, Fagg B, Stahel RA. Hematopoietic growth factors
387 secreted by seven human pleural mesothelioma cell lines: interleukin-6
388 production as a common feature. *Int J Cancer* 1992; 51: 296-301.
- 389 14. Stahel RA, O'Hara CJ, Waibel R, Martin A. Monoclonal antibodies against
390 mesothelial membrane antigen discriminate between malignant mesothelioma
391 and lung adenocarcinoma. *Int J Cancer* 1988; 41: 218-223.

- 392 15. Harsha HC, Molina H, Pandey A. Quantitative proteomics using stable isotope
393 labeling with amino acids in cell culture. *Nat Protoc* 2008; 3: 505-516.
- 394 16. Han DK, Eng J, Zhou H, Aebersold R. Quantitative profiling of
395 differentiation-induced microsomal proteins using isotope-coded affinity tags
396 and mass spectrometry. *Nat Biotechnol* 2001; 19: 946-951.
- 397 17. Li XJ, Zhang H, Ranish JA, Aebersold R. Automated statistical analysis of
398 protein abundance ratios from data generated by stable-isotope dilution and
399 tandem mass spectrometry. *Anal Chem* 2003; 75: 6648-6657.
- 400 18. Livak KJ, Schmittgen TD. Analysis of relative gene expression data using
401 real-time quantitative PCR and the 2⁻(Delta Delta C(T)) Method. *Methods*
402 2001; 25: 402-408.
- 403 19. Saalbach A, Aneregg U, Bruns M, Schnabel E, Herrmann K, Hausteil UF.
404 Novel fibroblast-specific monoclonal antibodies: properties and specificities. *J*
405 *Invest Dermatol* 1996; 106: 1314-1319.
- 406 20. Ong SE, Blagoev B, Kratchmarova I, Kristensen DB, Steen H, Pandey A,
407 Mann M. Stable isotope labeling by amino acids in cell culture, SILAC, as a
408 simple and accurate approach to expression proteomics. *Mol Cell Proteomics*
409 2002; 1: 376-386.
- 410 21. Ordonez NG. Application of mesothelin immunostaining in tumor diagnosis.
411 *Am J Surg Pathol* 2003; 27: 1418-1428.
- 412 22. Ordonez NG. Value of E-cadherin and N-cadherin immunostaining in the
413 diagnosis of mesothelioma. *Hum Pathol* 2003; 34: 749-755.
- 414 23. Ordonez NG. The immunohistochemical diagnosis of mesothelioma: a
415 comparative study of epithelioid mesothelioma and lung adenocarcinoma. *Am*
416 *J Surg Pathol* 2003; 27: 1031-1051.
- 417 24. Bagutti C, Forro G, Ferralli J, Rubin B, Chiquet-Ehrismann R. The
418 intracellular domain of teneurin-2 has a nuclear function and represses zic-1-
419 mediated transcription. *J Cell Sci* 2003; 116: 2957-2966.
- 420 25. Nathanson KL, Shugart YY, Omaruddin R, Szabo C, Goldgar D, Rebbeck TR,
421 Weber BL. CGH-targeted linkage analysis reveals a possible BRCA1 modifier
422 locus on chromosome 5q. *Hum Mol Genet* 2002; 11: 1327-1332.
- 423 26. Vinatzer U, Gollinger M, Mullauer L, Raderer M, Chott A, Streubel B.
424 Mucosa-associated lymphoid tissue lymphoma: novel translocations including
425 rearrangements of ODZ2, JMJD2C, and CNN3. *Clin Cancer Res* 2008; 14:
426 6426-6431.
- 427 27. Bradley JE, Ramirez G, Hagood JS. Roles and regulation of Thy-1, a context-
428 dependent modulator of cell phenotype. *Biofactors* 2009; 35: 258-265.
- 429 28. Cao Q, Abeysinghe H, Chow O, Xu J, Kaung H, Fong C, Keng P, Insel RA,
430 Lee WM, Barrett JC, Wang N. Suppression of tumorigenicity in human
431 ovarian carcinoma cell line SKOV-3 by microcell-mediated transfer of
432 chromosome 11. *Cancer Genet Cytogenet* 2001; 129: 131-137.
- 433 29. Abeysinghe HR, Cao Q, Xu J, Pollock S, Veyberman Y, Guckert NL, Keng P,
434 Wang N. THY1 expression is associated with tumor suppression of human
435 ovarian cancer. *Cancer Genet Cytogenet* 2003; 143: 125-132.
- 436 30. Abeysinghe HR, Pollock SJ, Guckert NL, Veyberman Y, Keng P, Halterman
437 M, Federoff HJ, Rosenblatt JP, Wang N. The role of the THY1 gene in human
438 ovarian cancer suppression based on transfection studies. *Cancer Genet*
439 *Cytogenet* 2004; 149: 1-10.

- 440 31. Lung HL, Cheng Y, Kumaran MK, Liu ET, Murakami Y, Chan CY, Yau WL,
441 Ko JM, Stanbridge EJ, Lung ML. Fine mapping of the 11q22-23 tumor
442 suppressive region and involvement of TSLC1 in nasopharyngeal carcinoma.
443 *Int J Cancer* 2004; 112: 628-635.
- 444 32. Lung HL, Bangarusamy DK, Xie D, Cheung AK, Cheng Y, Kumaran MK,
445 Miller L, Liu ET, Guan XY, Sham JS, Fang Y, Li L, Wang N, Protopopov AI,
446 Zabarovsky ER, Tsao SW, Stanbridge EJ, Lung ML. THY1 is a candidate
447 tumour suppressor gene with decreased expression in metastatic
448 nasopharyngeal carcinoma. *Oncogene* 2005; 24: 6525-6532.
- 449 33. Yang ZF, Ho DW, Ng MN, Lau CK, Yu WC, Ngai P, Chu PW, Lam CT,
450 Poon RT, Fan ST. Significance of CD90+ cancer stem cells in human liver
451 cancer. *Cancer Cell* 2008; 13: 153-166.
- 452 34. Liu G, Yuan X, Zeng Z, Tunici P, Ng H, Abdulkadir IR, Lu L, Irvin D, Black
453 KL, Yu JS. Analysis of gene expression and chemoresistance of CD133+
454 cancer stem cells in glioblastoma. *Mol Cancer* 2006; 5: 67.
- 455 35. Gupta PB, Onder TT, Jiang G, Tao K, Kuperwasser C, Weinberg RA, Lander
456 ES. Identification of selective inhibitors of cancer stem cells by high-
457 throughput screening. *Cell* 2009; 138: 645-659.
- 458 36. Melotti A, Daga A, Marubbi D, Zunino A, Mutti L, Corte G. In vitro and in
459 vivo characterization of highly purified human mesothelioma derived cells.
460 *BMC Cancer*; 10: 54.

461

462

463

464

465

466

467

468

469

470

471

472

473

474

475

476

477

478 **Legends for figures**

479 **Figure 1.** *Workflow for the identification and verification of MPM discriminatory*
480 *marker candidates.* Cell surface capturing (CSC) was applied in combination with
481 SILAC for quantitative analysis of the N-glycosylated cell surface proteins of the
482 MPM cell line ZL55 and the ADCA cell line Calu-3. Differentially regulated proteins
483 were investigated by LDA assays on a panel of MPM and ADCA cell lines. Proteins
484 showing potential specificity for MPM were verified at cell and tissue level by
485 antibody-based assays.

486 **Figure 2.** *Detection and quantitation of the reference mesothelioma markers*
487 *mesothelin and N-cadherin.* **A,** Mass spectrometric quantitation of the mesothelin
488 peptide LAFQNMNGSEYFVK and N-cadherin peptide VDIIVANLTVTDK
489 identified by CSC in the SILAC-heavy-labelled MPM cell line ZL55 and the light-
490 labelled ADCA cell line Calu-3. The XPRESS software was used to define the elution
491 areas of the peptides and calculate the isotopic ratios between light and heavy peptide
492 forms. Elution areas used for quantitation are delimited by the dotted blue curves
493 between the dashed black-lines. The red traces are the peptide chromatograms
494 identified in the elution areas used for quantitation. **B,** Western blot detection of
495 mesothelin and N-cadherin. Reaction against the anti-mesothelin antibody can be
496 detected for the MPM cell line ZL55, but is only weak or absent for the ADCA cell
497 line Calu-3. Similar can be observed using the anti-N-cadherin antibody.

498 **Figure 3.** *Mass spectrometric quantitation of the proteins thy-1/CD90 and teneurin-2*
499 *and relative mRNA expression as assessed by low density array RT-PCR profiling.* **A,**
500 Elution profiles of the thy-1/CD90 peptide SPPISSQNVTVLR and the teneurin-2

501 peptide NSSIDSGEAEVGR identified by CSC of the heavy-labeled MPM cell line
502 ZL55 and the light-labeled ADCA cell line Calu-3. Quantitation was calculated with
503 the software XPRESS and derived from the isotopic ratios of the elution areas of the
504 peptides. Dotted blue curves between the dashed black-lines mark elution areas used
505 for relative quantitation. The red traces correspond to the peptide chromatograms
506 identified in the elution areas used for quantitation. B, Graphs show the relative
507 mRNA levels of mesothelin (gene name MSLN), N-cadherin (gene name CDH2),
508 thy-1/CD90 (gene name THY1) and teneurin-2 (gene name ODZ2) in fifteen MPM
509 (dashed bars, cell lines ZL55 to SDM61) and six ADCA (black bars, cell lines Calu-3
510 to SK-LU-1) cell lines.

511 **Figure 4.** *Expression of thy-1/CD90 protein in MPM and ADCA cell lines.* Protein
512 lysates from ADCA cell lines Calu-3 and SK-LU-1 and from MPM cell lines ZL55
513 and SDM5 were separated on SDS-PAGE (4-12%). For deglycosylation, cell lysates
514 were treated with PNGaseF. Using mouse anti-thy-1 antibody, a band compatible with
515 the size of thy-1/CD90 (28 kDa) was detected in the untreated SDM5 lysates. Upon
516 PNGaseF treatment, signals at 17 kDa were detected in both MPM cell lines, which
517 agree with the weight of deglycosylated thy-1/CD90. Independent of PNGaseF
518 treatment, no signal could be detected for the ADCA cell lines. The position of
519 weight standards is indicated at the left, while - *and* + indicate lysates without and
520 with PNGaseF treatment, respectively.

521 **Figure 5.** *Immunofluorescent and immunohistochemical detection of thy-1/CD90.*

522 **A,** Immunofluorescent staining of thy-1/CD90 protein in MPM and ADCA cell lines.
523 The MPM cell line ZL55 and the ADCA cell line Calu-3 were stained with mouse
524 anti-thy-1 antibody 5E10 (red). Cell membranes were counterstained with Alexa

525 Fluor 488-conjugated cholera-toxin (green), and nuclei with DAPI (blue). Merged
526 images are shown at the far right. **B**, Two representative IHC examples of human
527 MPM (*a-b*) and ADCA (*c-d*). Images were recorded at *10x* and representative regions
528 (insets) at *20x* magnification. Reference slides from the same tumors were also
529 stained with haematoxylin-eosin.

530

531

532

533

534

535

536

537

538

539

540

541

542

543

544

545

546

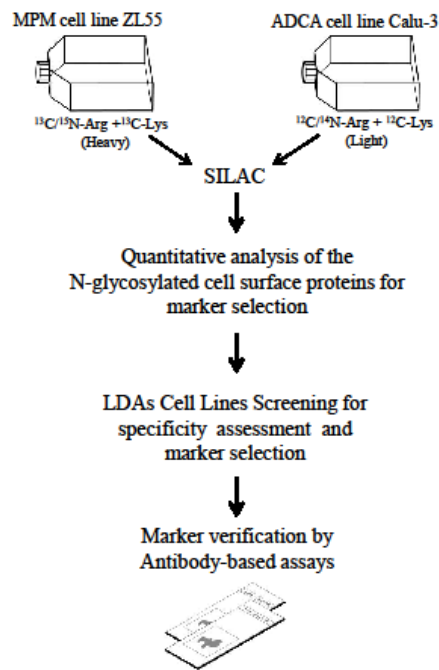
547

548

549

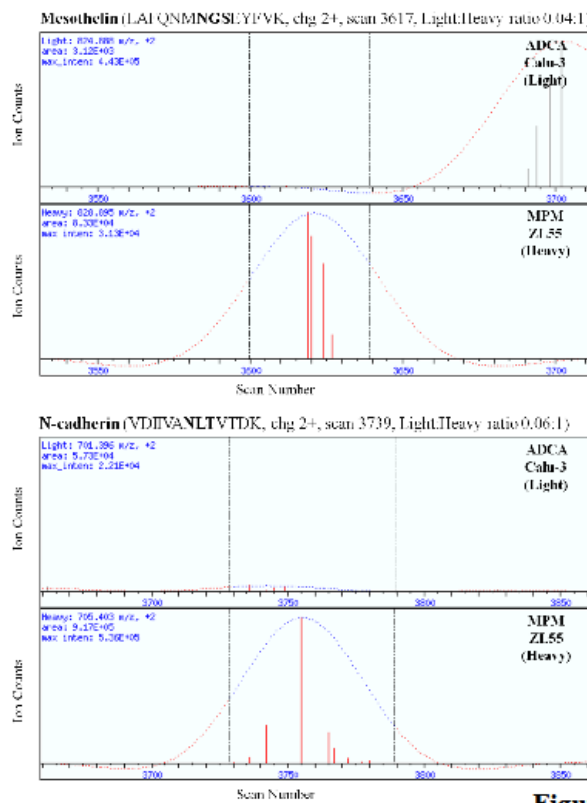
550 **Table 1: Cell lines used for LDAs assays**

Cell line	Type	Histology	Origin	Patient (sex/age)	Source/Reference
ZL55	MPM	Epithelioid	Tumor	M/52	Our lab, <i>ref.13</i>
SDM5	MPM	Epithelioid	Effusion	M/54	Our lab
SDM13	MPM	Epithelioid	Tumor	M/58	Our lab
SDM16	MPM	Epithelioid	Tumor	M/65	Our lab
SDM22	MPM	Epithelioid	Effusion	M/62	Our lab
SDM46	MPM	Epithelioid	Tumor	M/57	Our lab
SDM47	MPM	Epithelioid	Tumor	M/58	Our lab
SDM48	MPM	Epithelioid	Tumor	M/55	Our lab
SDM55	MPM	Epithelioid	Tumor	M/40	Our lab
SDM57	MPM	Epithelioid	Tumor	F/62	Our lab
SDM61	MPM	Epithelioid	Tumor	M/66	Our lab
MSTO-211H	MPM	Biphasic	Effusion	M/62	Our lab
H2052	MPM	Sarcomatoid	Effusion	M/65	ATCC
H2452	MPM	Epithelioid	Tumor	M/-	ATCC
H226	MPM	Epithelioid	Effusion	M/-	ATCC
Calu-3	NSCLC	ADCA	Effusion	M/25	ATCC
Calu-6	NSCLC	ADCA	-	F/61	ATCC
A549	NSCLC	ADCA	-	M/58	ATCC
SK-LU-1	NSCLC	ADCA	-	F/60	ATCC
ZL25	NSCLC	ADCA	-	M/60	Our lab, <i>ref.14</i>
H596	NSCLC	Adenosquamous	-	M/73	ATCC



552

Figure 1, Ziegler, Cerciello et al.



553

Figure 2A, Ziegler, Cerciello et al.

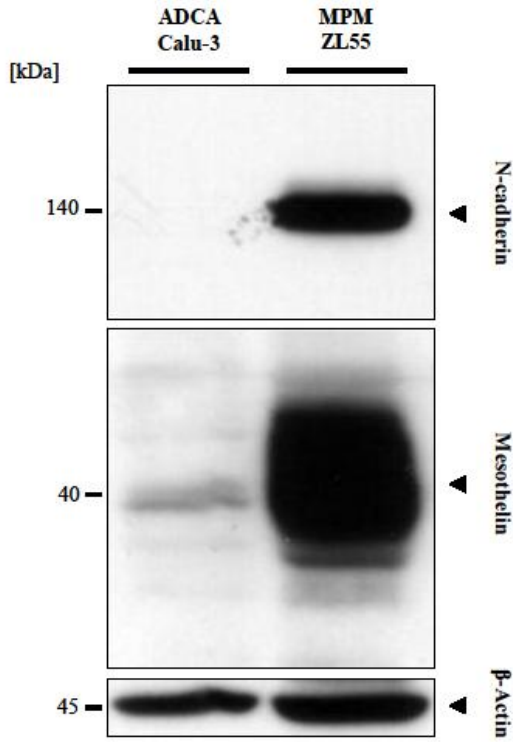


Figure 2B, Ziegler, Cerciello et al.

554

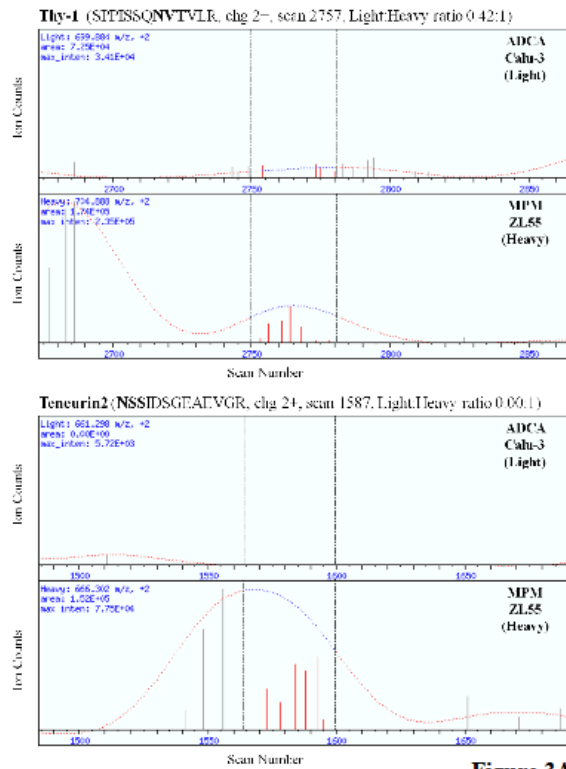


Figure 3A, Ziegler, Cerciello et al.

555

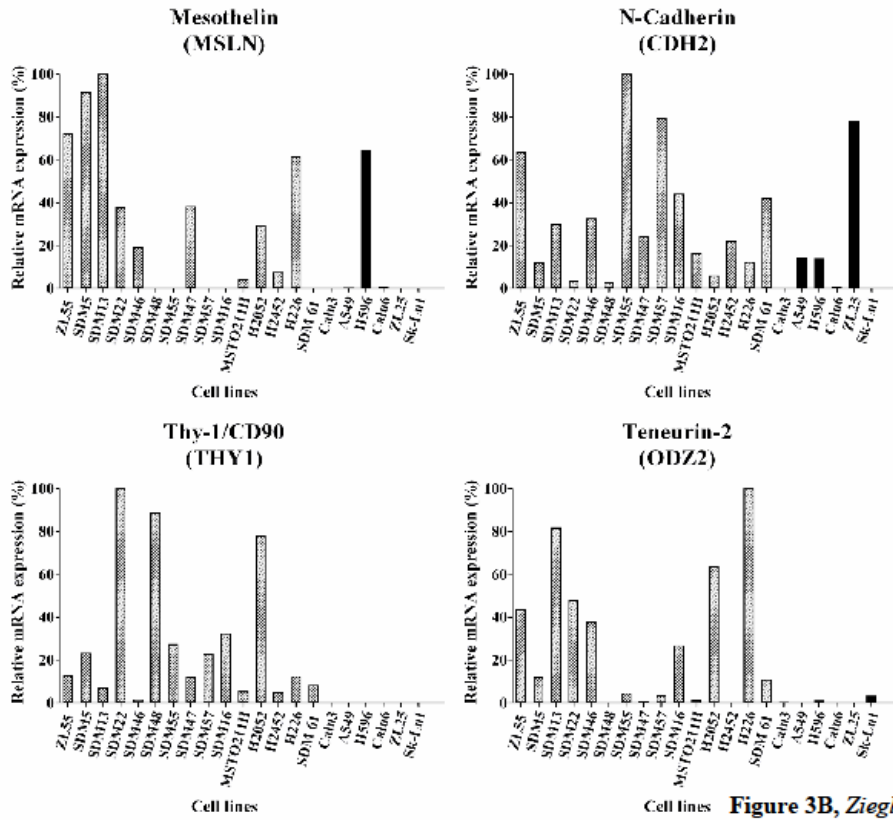


Figure 3B, Ziegler, Cerciello et al.

556

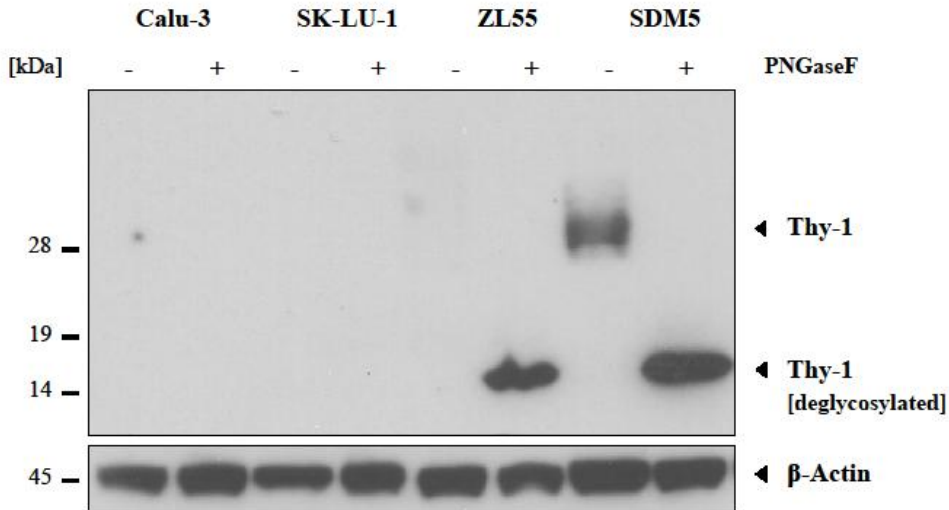
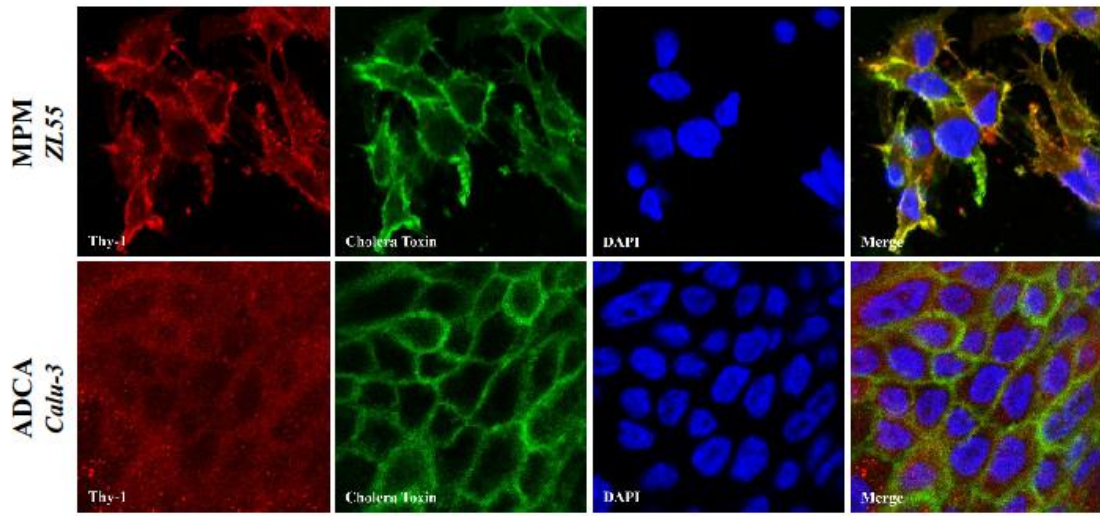


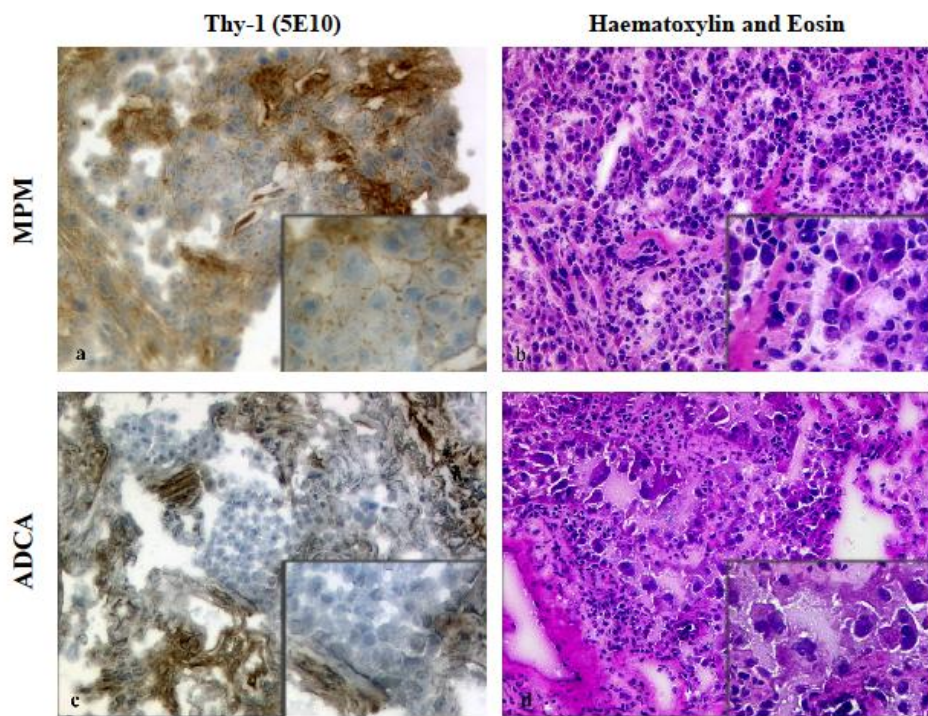
Figure 4, Ziegler, Cerciello et al.

557



558

Figure 5A, Ziegler, Cerciello et al.



559

Figure 5B, Ziegler, Cerciello et al.